


# Neuromonitoring During Robotic Cochlear Implantation: Initial Clinical Experience

JUAN ANSÓ,<sup>1</sup> OLIVIER SCHEIDEGGER,<sup>2</sup> WILHELM WIMMER <sup>1,3</sup> KATE GAVAGHAN,<sup>1</sup> NICOLAS GERBER,<sup>1</sup> DANIEL SCHNEIDER,<sup>1</sup> JAN HERMANN,<sup>1</sup> CHRISTOPH RATHGEB,<sup>1</sup> CILGIA DÜR,<sup>1,3</sup> KAI MICHAEL RÖSLER,<sup>2</sup> GEORGIOS MANTOKOUDIS,<sup>1,3</sup> MARCO CAVERSACCIO,<sup>1,3</sup> and STEFAN WEBER<sup>1</sup>

<sup>1</sup>ARTORG Center for Biomedical Engineering, University of Bern, Murtenstrasse 50, 3008 Bern, Switzerland; <sup>2</sup>Department of Neurology, Inselspital, University of Bern, Bern, Switzerland; and <sup>3</sup>Department of Head and Neck Surgery, Inselspital, University of Bern, Bern, Switzerland

(Received 20 February 2018; accepted 11 July 2018; published online 26 July 2018)

Associate Editor Cameron N. Riviere oversaw the review of this article.

**Abstract**—During robotic cochlear implantation a drill trajectory often passes at submillimeter distances from the facial nerve due to close lying critical anatomy of the temporal bone. Additional intraoperative safety mechanisms are thus required to ensure preservation of this vital structure in case of unexpected navigation system error. Electromyography based nerve monitoring is widely used to aid surgeons in localizing vital nerve structures at risk of injury during surgery. However, state of the art neuromonitoring systems, are unable to discriminate facial nerve proximity within submillimeter ranges. Previous work demonstrated the feasibility of utilizing combinations of monopolar and bipolar stimulation threshold measurements to discretize facial nerve proximity with greater sensitivity and specificity, enabling discrimination between *safe* ( $> 0.4$  mm) and *unsafe* ( $< 0.1$  mm) trajectories during robotic cochlear implantation (*in vivo* animal model). Herein, initial clinical validation of the determined stimulation protocol and nerve proximity analysis integrated into an image guided system for safety measurement is presented. Stimulation thresholds and corresponding nerve proximity values previously determined from an animal model have been validated in a first-in-man clinical trial of robotic cochlear implantation. Measurements performed automatically at preoperatively defined distances from the facial nerve were used to determine safety of the drill trajectory intraoperatively. The presented system and automated analysis correctly determined sufficient safety distance margins ( $> 0.4$  mm) to the facial nerve in all cases.

**Keywords**—Image-guided, Electromyography, Facial nerve, Stimulation, Multipolar, Bipolar, Safety, Submillimeter, Accuracy.

Address correspondence to Wilhelm Wimmer, ARTORG Center for Biomedical Engineering, University of Bern, Murtenstrasse 50, 3008 Bern, Switzerland. Electronic mail: wilhelm.wimmer@artorg.unibe.ch

## INTRODUCTION

Robotic cochlear implantation (RCI), as described in detail by Caversaccio and Weber *et al.*,<sup>8,25</sup> involves the image-guided drilling of a minimally invasive tunnel access to the inner ear for electrode insertion into the cochlea. Due to the close proximity of critical micro-anatomy contained within the temporal bone, robotic drilling through the facial recess is often planned and carried out at submillimeter distances from the facial nerve (FN). Despite the high accuracy and reliability of systems performing the procedure,<sup>6</sup> safety measures that ensure preservation of this critical structure, even in cases of unexpected system or operation error, are required. A measure of facial nerve location relative to the approaching drill that is independent of the image guidance model could detect a drill trajectory passing at an unsafe distance from the nerve and prevent penetration and functional damage to the nerve tissue.

Electromyography (EMG) based facial nerve monitoring (FNM) is a commonly used tool for locating the facial nerve during surgical procedures on the lateral skull base.<sup>12</sup> The activity of the facial nerve is monitored *via* needle measurement electrodes implanted in the innervated facial muscles. Two types of EMG activity may be recorded and monitored during surgery<sup>13,16</sup>: free-running EMG and stimulated EMG.

Free-running EMG, as employed by Labadie *et al.* during the first cases of minimally invasive cochlear implantation,<sup>17</sup> monitors background activity of the nerve and may identify scenarios of low anesthesia or

nerve irritation due to, for example, mechanical manipulation or induced temperature gradient (e.g., resulting from high-speed drilling or irrigation/cooling).<sup>14,19,21</sup> However, the utilization of free-running EMG to prevent iatrogenic nerve injury provides limited sensitivity, as anticipated by Holland *et al.*,<sup>13</sup> and later experienced by Labadie *et al.*<sup>17</sup>

Stimulated EMG relies on the application of electrical stimulation pulses *via* a (cathode) stimulating electrode to excite and localize a motor nerve at risk of injury during surgery. If the stimulating pulse has sufficient energy (amplitude and duration), the membrane resting potential of each nerve axons in the region of the excitation will be stimulated. A compound muscle action potential resulting from the synchronized activation of multiple motor unit potentials is measured in the innervated muscle allowing the minimum stimulation intensity (stimulus threshold) required to excite the nerve to be determined. A stimulation threshold of 1 mA is typically associated with 1 mm of remaining bone tissue between the stimulating electrode and the nerve.<sup>21</sup> Thus, measurements of stimulation threshold can be used to map the course of the facial nerve within the mastoid bone.

For nerve mapping based on stimulus-triggered EMG, two stimulating configurations (monopolar and bipolar) have been described.<sup>21</sup> Bipolar stimulation provides a focus stimulating current field between the two stimulating electrodes (effective interelectrode distance range from 2 to 4 mm).<sup>21</sup> However, if the portion of nerve of interest is embedded in bone, as is the case during cochlear implantation (CI) surgery, the generated electrical field *via* a bipolar stimulating electrode probe may not be sufficient.<sup>15</sup> During conventional surgery, monopolar stimulation is therefore chosen because it provides higher sensitivity.<sup>23</sup> FNM based on monopolar stimulation, however, lacks sufficient localization accuracy at submillimeter distances from the FN as required during RCI. Hence, conventional FNM systems have demonstrated insufficient sensitivity and specificity for RCI, with reported variances in nerve proximity measurement accuracies of up to 2 mm.<sup>4</sup>

To this end, our team previously developed a neuromonitoring approach based on facial nerve stimulation specifically for use during RCI.<sup>3</sup> By combining stimulus threshold measurements from a multipolar stimulating probe with predefined specific electrical field profiles, discretization of facial nerve proximity at the resolutions relevant to RCI was achieved. In an animal model,<sup>3</sup> stimulation protocol and stimulus threshold analysis that distinguished *safe* ( $> 0.4$  mm) and *unsafe* ( $< 0.1$  mm) distance regions from a

robotically drilled tunnel to the facial nerve, with sensitivity and specificity greater than 95%, were established. If a trajectory would lead to a distance to the facial nerve between 0.1 and 0.4 mm, the FNM approach may not identify this distance region with sensitivity and specificity greater than 95%.

Herein, a clinically applicable model of the previously established FNM approach for RCI is presented. A system for specific and automated nerve stimulation is presented along with methodologies of EMG response analysis. Validation of the approach for determining facial nerve proximity and safety during the initial ( $n = 7$ ) cases of a *first-in-man* RCI clinical trial is presented.

## MATERIALS AND METHODS

### *Neuromonitoring System and Approach*

The neuromonitoring system is composed of: (i) a multipolar navigated stimulating probe, (ii) two pairs of needle electromyogram electrodes, (iii) one pair of surface stimulating electrodes, (iv) an electrical nerve stimulation and monitoring system (ISIS, inomed), and (v) an application software for stimulation control, EMG monitoring and stimulus threshold analysis.

### *Multipolar Stimulating Probe*

The multipolar stimulating probe is composed of one cathode electrode (C) at the tip and three anode rings ( $A_i = 1,2,3$ ) distally located at distances  $d$  ( $d_i = 2,4,7$  mm) as described in Ref. 3 (Fig. 1). The smaller area of the cathode (C) electrode ( $0.4 \text{ mm}^2$ ) compared to the anode counter electrode ( $5.6 \text{ mm}^2$ ) provides a focus electrical field (volume conductor) around the tip of the probe with approximately 3 mm radius at 90% field attenuation (analysis not reported in this manuscript). Preclinical validations<sup>3</sup> demonstrated that electrical stimulation between the cathode and the anode rings (bipolar configurations) provide higher specificity to discriminate nerve proximity than monopolar stimulation. Lateral and frontal discrimination is not suitable given the concentric design of the stimulating probe.

### *Neuromonitoring Approach*

An EMG-based FNM approach has been developed to mitigate against the risk of structural damage to the facial nerve (Fig. 2). The FNM approach is composed of: (1) positive control, (2) free-running EMG and (3) multipolar stimulation of the facial nerve.

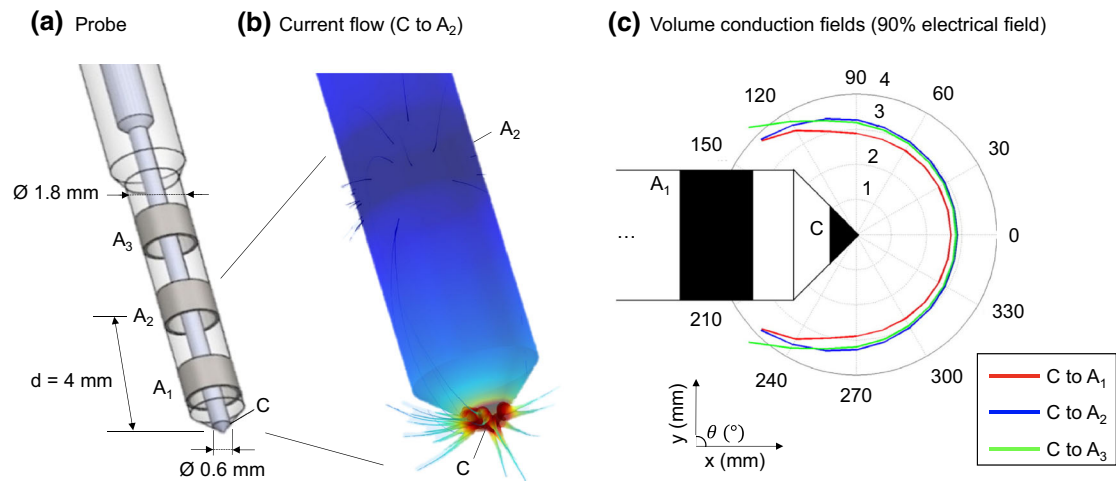


**FIGURE 1.** Multipolar stimulating probe. (a) Stimulating electrodes, with the cathode (C) and the three ring anodes ( $A_1$ ... $A_3$ ). (b) Current stream lines flowing from the cathode to one of the anodes ( $A_2$ ). (c) Volume conduction field of the different stimulating configurations of the probe, following approximately a 3 mm spherical shape around the cathode tip at 90% field decay (simulations not published).

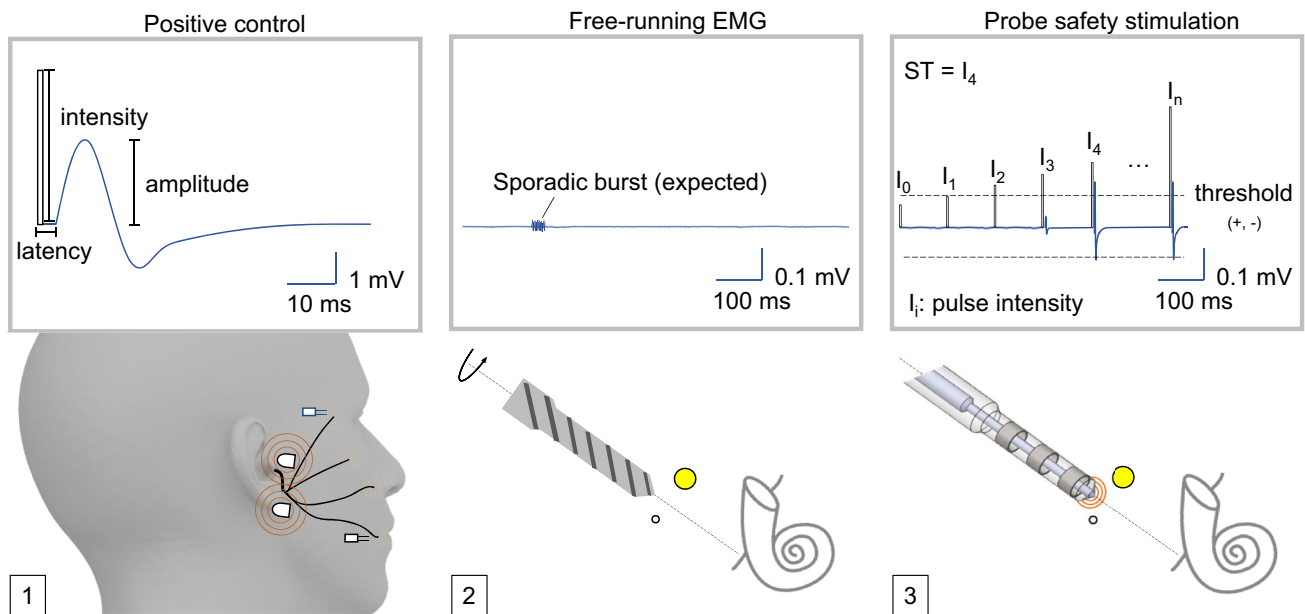


**FIGURE 2.** Facial nerve monitoring approach. (1) Positive control as applied through external surface electrodes with the elicited muscular activity represented in each innervated facial muscle. Two measuring needles are positioned to detect the electromyogram signals. (2) Free-running EMG as monitored during drilling of the tunnel. (3) Bipolar and monopolar stimulation to assess safety distance margins based on a train of pulse intensities ( $I_i$ ) and resulting stimulus thresholds.

### Positive Control

The EMG-based neuromonitoring system relies on the sensitivity of measuring EMG needle electrodes implanted in the facial muscles of the subject before the patient is draped. To assess sufficient sensitivity of the EMG needles, a *positive control* stimulation is applied via a pair of surface electrodes positioned near the exit of the main trunk of the facial nerve via the stylo-

mastoid foramen. Stimulus thresholds between 20 and 50 milliampere (monophasic stimulation pulse with 250  $\mu$ s duration) are expected in this region. Sufficient sensitivity of each EMG channel during the *positive control* is defined as a compound muscle potential with peak amplitudes above 100 microvolts.<sup>7,9</sup> If an EMG channel provides insufficient sensitivity ( $< 100 \mu$ V) to the threshold stimulation, the corresponding measuring needles must be repositioned in the muscle.

### Free-Running EMG

Functional nerve status is continuously monitored *via* non-electrically triggered EMG (free-running EMG) responses. Although its sensitivity is limited, free-running EMG may support in identification of nerve irritation (neurotonic discharges) due to, for example, excessive mechanical pressure or temperature rise. During free-running electromyography larger time scan windows ( $\sim$  seconds) than in stimulus-triggered EMG ( $\sim$  100 ms) are used to ensure visualization of background nerve activity (e.g., high frequency bursts). Signal peak amplitudes during free-running EMG are typically lower ( $\sim$  50  $\mu$ V)<sup>13</sup> than during stimulus-triggered electromyography. In Fig. 3, a semi-rhythmic EMG response is depicted. This kind of EMG spontaneous activity is rare during robotic cochlear implantation and it should not be misinterpreted with ambient interference noise from external electrically powered instruments (e.g., tracking system spikes with similar repetition rate and amplitude). During robotic drilling between the facial nerve and the chorda tympani (Fig. 3b), sporadic low energy EMG bursts ( $\sim$  50  $\mu$ V) may be monitored.

### Multipolar Stimulation for Safety Facial Nerve Distance Assessment

By measuring EMG signals in the facial muscles induced by electrical stimulation of the facial nerve through the stimulating probe, the distance of the tra-

jectory to the facial nerve can be estimated. Stimulation points along the planned drill trajectory within close proximity the facial nerve (FNM points) are preoperatively planned at specific distances from the nerve (Fig. 4). During drilling, on reaching each point, the robot automatically evacuates from the drill tunnel, followed by manual insertion of the stimulation probe. An automatic stimulus threshold search is applied to each of the electrode configurations of the inserted stimulation probe. From previous experimental calibration<sup>3</sup> stimulus threshold values above 1 mA (monopolar) are hypothesized to indicate that the remaining bone thickness between the drill trajectory and the facial nerve is sufficiently protective, whereas values below 0.3 mA (bipolar) may indicate facial nerve dehiscence or absence of nerve bone covering possibly due to drill breaking through the bony canal enveloping the nerve.

### Definition of FNM Stimulus Points for Safety Assessment

The origin of the ( $N = 5$ ) FNM points (Table 1) is defined as the minimum distance from the center line of the segmented facial nerve to the axis of the planned trajectory (Fig. 4). A first FNM measurement point ( $P_1$ ) is located at a distance  $L_1$  before the projected FN center origin. The last FNM point ( $P_N$ ) is located at a distance  $L_N$  beyond the origin. The distance between two consecutive FNM points is determined *via* the following linear equation (1)

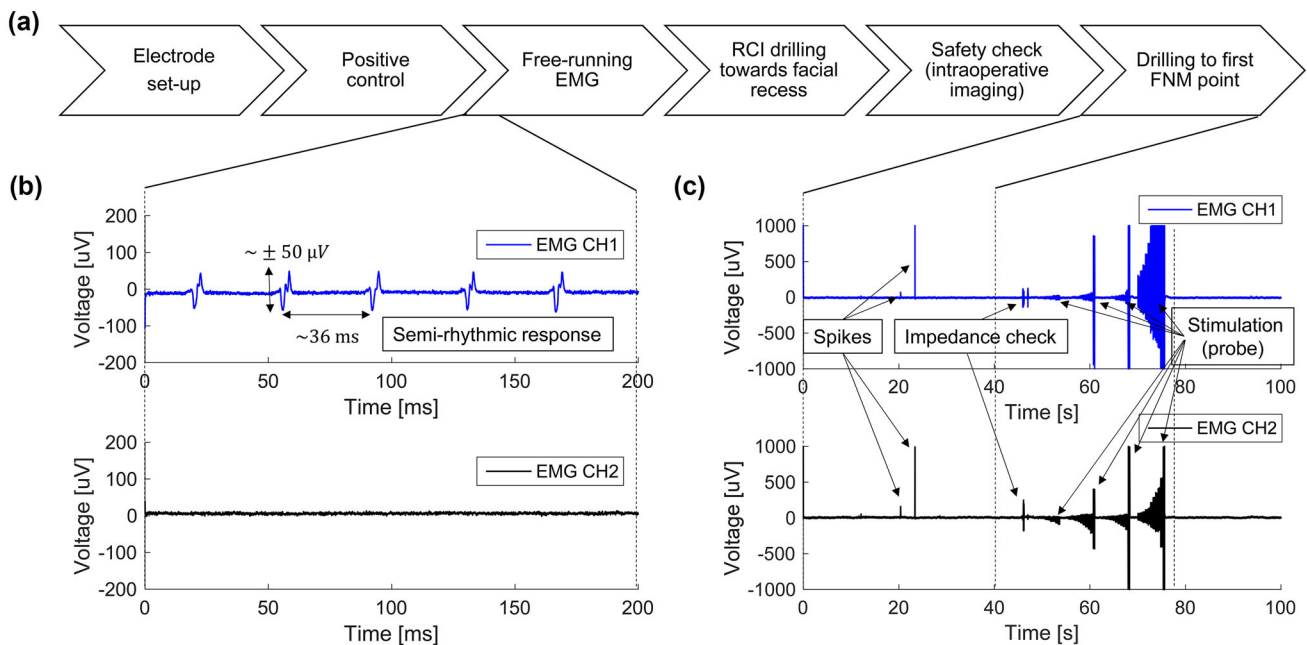


**FIGURE 3.** (a) Facial nerve monitoring workflow as it is related to the robotic drilling before reaching a first probe-based stimulation point. (b) A semi-rhythmic electromyogram response observed during free-running EMG, likely due to low anesthesia phase (Patient 1). (c) Longer capture of the free-running signals depicting (Patient 3): (1) spikes from technical equipment, (2) artifacts from impedance check (stimulation electrodes) prior to application of probe stimulation (four channels).

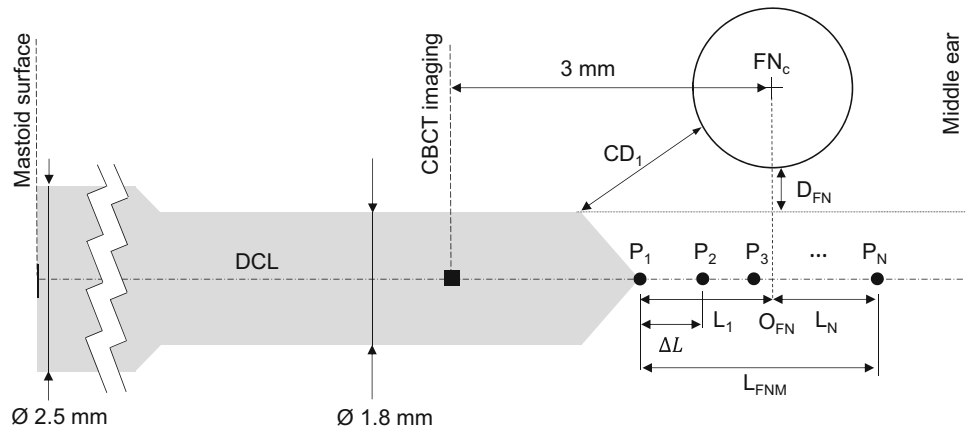


**FIGURE 4.** Definition of neuromonitoring points relative to the facial nerve along the drill center line (trajectory axis). The drill is represented as it reached the first FNM point with closest distance  $CD_1$ . The distance increment ( $\Delta L = 0.54$  mm) between measuring points  $P_1$  and  $P_2$  is depicted. The diameter of the drill and an intraoperative safety measurement point (3 mm before the FN origin) (cone beam computed tomography CBCT imaging) are represented. The final drill-to-facial nerve distance is represented as the distance from the surface of drilled tunnel to the nerve canal  $D_{FN}$ .

**TABLE 1.** Description of nomenclature of the measuring model to assess nerve proximity.

Term	Description
DCL	Axis of the drill trajectory or drill center line
$FN_C$	FN center point in the minimum distance plane between the FN center line and the RCI trajectory
$O_{FN}$	Origin of the facial nerve projected onto the RCI drill trajectory
$N$	Number of FNM measurement points
$L_{FNM}$	Length along the facial recess segment with FNM measurement points
$P_i$	FNM measurement points along the length $L_{FNM}$
$L_1$	Distance from $O_{FN}$ to the first FNM measurement point $P_1$
$L_n$	Distance from $O_{FN}$ to the last FNM measurement point $P_N$
$\Delta L$	Distance between two consecutive FNM measurement points
$CD_i$	Euclidian distance from the drilled tunnel (surface) to the FN at each measuring point $P_i$
$D_{FN}$	Postoperative lateral distance from the trajectory to the FN along the DCL

$$\Delta L = \frac{L_{FNM}}{N} = \frac{L_1 + L_N}{N} \quad (1)$$

The diameter of the facial nerve may vary from 1.7 to 2.3 mm ( $1.97 \pm 0.26$  mm)<sup>24</sup> (expected FN radius from 0.85 to 1.15 mm). Thus, to enable detection of the FN boundary in case of unexpected navigation error,  $P_1$  is defined at ( $L_1$ ) 1.2 mm before reaching the origin of the FN in the drill axis ( $O_{FN}$ ) (Fig. 4). The last measurement point  $P_N$  is defined as an offset ( $L_N$ ) of 0.9 mm (length of the drill bit tip), enabling a last FNM measurement after passing the FN center. Between the first and last measurement points,  $N-2$  linearly distributed points are defined at axial increments  $\Delta L$  of 0.54 mm ( $\Delta L = \frac{1.2+0.9}{5}$ ).

### Clinical Trial

With approval from the local institutional review board (Ethics Committee of the Canton of Bern, Switzerland, KEK-BE 156/13, PB\_2017-00312) and

national medical device regulatory body (Swissmedic 2013-MD-0042, EUDAMED CIV-13-12-011779), a clinical trial on the feasibility of the robotic approach commenced in June 2016<sup>8,25</sup> at the University Hospital of Bern, Switzerland. Adult patients were asked for consent after screening of the facial recess size with a minimum distance requirement of 2.5 mm from the FN to the chorda, as described in Refs. 8 and 26. One day prior to surgery, a preoperative base line assessment of the facial nerve was conducted. Prior to commencement of the robotic surgery, each patient was implanted with four fiducial screws ( $\emptyset 2.2 \times 5$  mm length, M-5243.05, Medartis) in the mastoid to enable later physical registration of the robot and patient's coordinate systems. A high resolution ( $0.156 \times 0.156$  mm<sup>2</sup>, slice thickness 0.2 mm) computed tomography (CT) scan of the mastoid was obtained (SOMATOM, definition Edge, Siemens, Erlangen, Germany) and a plan created as described by Gerber *et al.*<sup>10</sup>

### Site Preparation and EMG Set-Up

A surgical system for robotic cochlear implantation described in Weber *et al.*<sup>25</sup> was installed in the side rails of the operation bed. The system enables image-guided accurate drilling of the preoperative planned trajectory from the mastoid surface to the entrance of the cochlea. The system relies on accurate fiducial registration (error < 0.1 mm)<sup>11</sup> and process navigation (visual servoing) to ensure target accuracies below 0.2 mm at the target.<sup>6</sup> The patient's head was accommodated and fixed to the operation table *via* a non-invasive headrest system with pressurized pads.

Prior to the commencing surgery, two pairs of subdermal needles (12 × 0.4 mm, Neuroline twisted pair, Ambu) were inserted in the facial muscles (orbicularis oculi labeled as EMG CH1 and oris as EMG CH2) of the RCI site (Fig. 5a). A pair of surface stimulation electrodes (23 × 23 mm, self-adhesive, in-omed) were attached near the superficial trunk of the facial nerve along its anatomical path in front of the external ear. Stimulation intensity was applied through the *positive control* stimulating electrodes until EMG peak amplitudes over threshold (> 100  $\mu$ V) were observed. Upon verification of sufficient EMG amplitude and acceptable base-line measuring noise (< 10  $\mu$ V peak) in the EMG signals, the patient's site was draped.

### Robotic Drilling and Free-Running EMG

The registration of the patient's mastoid to the image based surgical plan was realized using the fiducial screws and a registration instrument described in Ref. 11. RCI drilling was then commenced (Fig. 5b) while free-running EMG was monitored. The first drilling phase continued until a predefined safety check point, 3 mm before reaching the facial nerve (Fig. 4).<sup>25</sup>

Intraoperative evaluation of the drilled axis relative to the facial nerve was then carried out using a cone-beam CT (CBCT) imaging system (0.3 mm isotropic, xCAT, Xoran, USA). After initial intraoperative safety assessment of distance margins to the facial nerve (> 0.3 mm) and chorda tympani (> 0.2 mm), the critical drilling phase through the facial recess commenced. Free-running EMG monitored any signs of nerve activity while the surgical robot drilled to each subsequent stimulated FNM point.

### Safety Distance Assessment from Multipolar FN Stimulation

On reaching the first FNM point ( $P_1$ ), the robot guided drill retracted from the tunnel and the surgeon inserted the (navigated) probe *via* “press-fit” after application of ringer solution (NaCl, 0.9%) (Fig. 6). The “press-fit” insertion of the probe is facilitated by manufacturing tolerances with diameters of the distal elements of the probe a few micrometers thinner than the RCI drill. The probe was optically tracked during EMG measurements to confirm correct placement at the end of the tunnel.

After verification of sufficient electrode-contact impedance ( $Z_{Ai} < 20 \text{ k}\Omega$ ), a stimulus threshold search is carried out *via* a train of stimulation pulses (monophasic, 250- $\mu$ s duration, 0.2 to 2.5 mA, logarithmic, two repetitions/amplitude) applied at 4 Hz frequency for each configuration of the probe. The FNM system provided a binary safety classification based on the critical threshold of 0.3 mA (look up table defined in Table 2), as suggested from previous *in vivo* trials.<sup>3,25</sup> The look-up table is an idealized digital representation of five potential binary safety outputs (states) that could be expected based on the critical stimulus threshold of 0.3 mA:

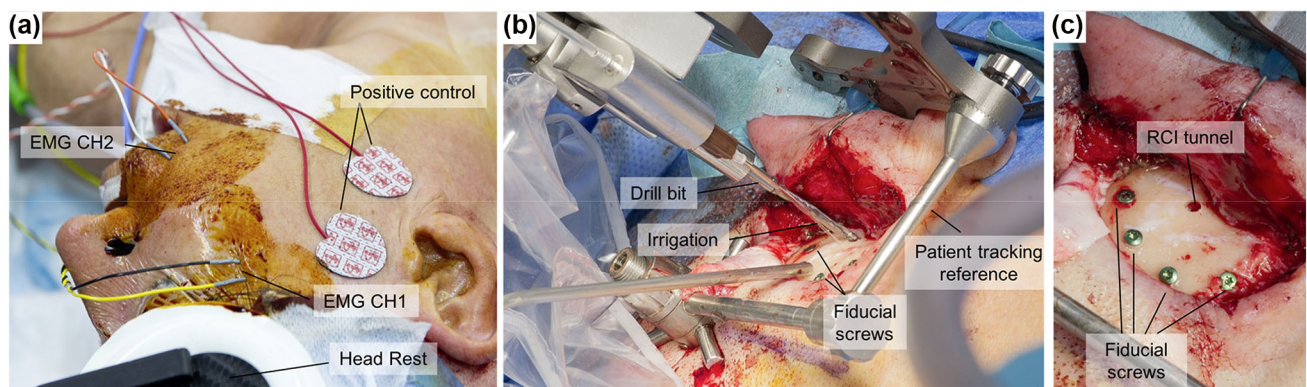


**FIGURE 5.** Facial nerve monitoring electrode set-up, robotic drilling and drilled tunnel (Patient 5). (a) The EMG needle electrodes (channels CH1, CH2) and the *positive control* stimulating (surface) electrodes are depicted. (b) The robotic drilling to the next FNM measurement point with the drill bit being irrigated during the drilling process. (c) The RCI drilled tunnel before inserting the stimulating FNM probe.

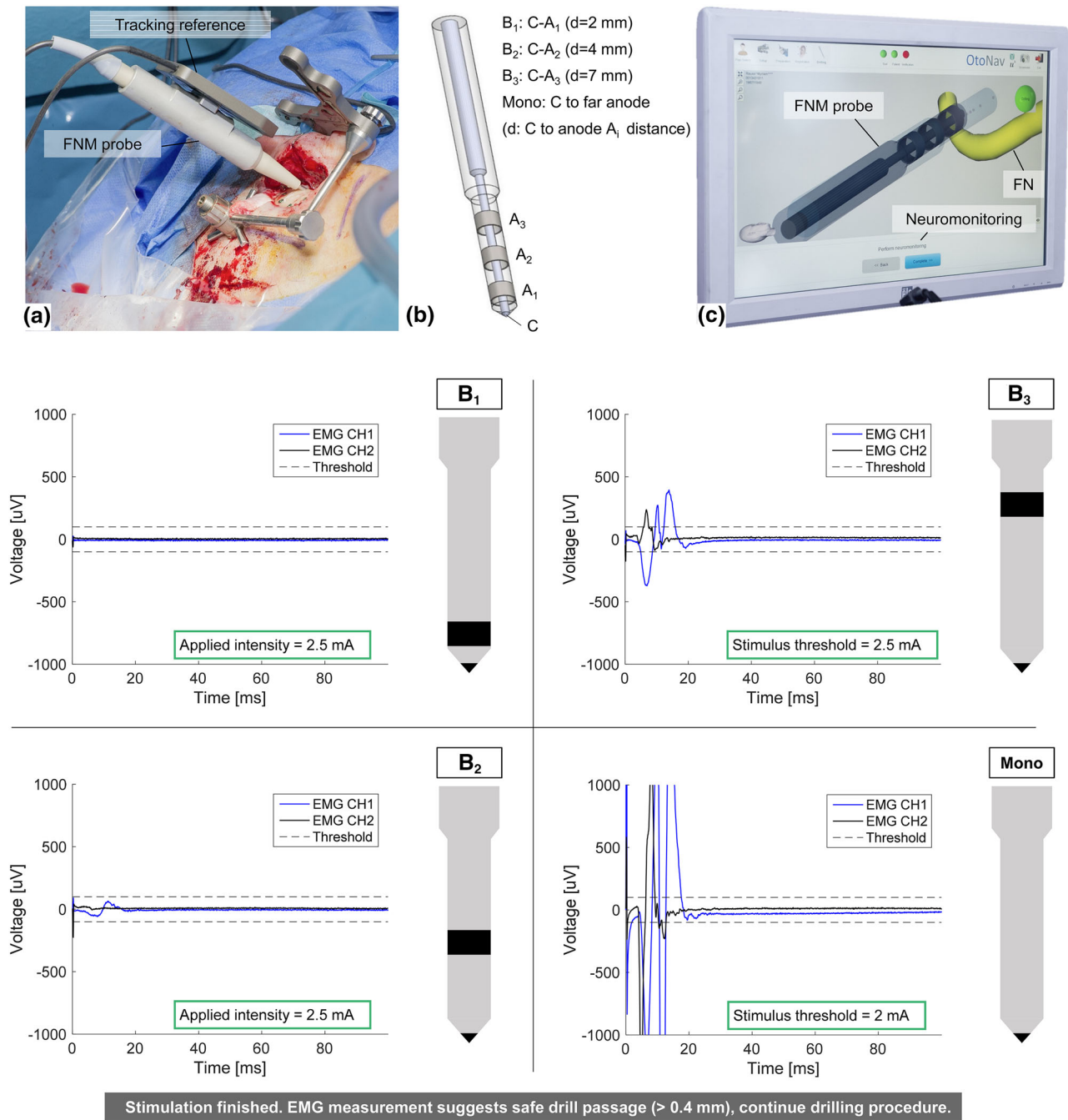


**FIGURE 6.** Safety distance assessment based on facial nerve monitoring. On the top panel: (a) The stimulating probe as inserted to the end of the drilled tunnel. (b) The stimulating electrodes of the probe depicting each of the four cathode-to-anode combinations ( $B_1$ ,  $B_2$ ,  $B_3$  and monopolar). (c) Visual feedback of the tracked stimulation probe once inserted into the next FNM point. In the bottom panel: Intraoperative analysis of stimulus thresholds as presented to the user (Patient 3, measuring point  $P_1$ ). After automatic search of the stimulus thresholds for each of the four stimulation channels, the system presents the electromyogram signals and intensity thresholds to the user. The user carries out verification to ensure the suggested thresholds are no artifacts (no false positives/negatives).

- (i) States 0–2: Continue to drill (FN distance  $> 0.4$  mm, confidence  $> 95\%$ )
- (ii) State 3: Further assessment ( $0.1 < \text{FN distance} < 0.4$  mm, confidence  $< 95\%$ )

- (iii) State 4: Abort RCI (FN distance  $< 0.1$  mm, confidence  $> 95\%$ )

If a stimulus threshold of  $0.3$  mA is assessed with the bipolar configuration  $B_1$ , equal or lower stimulus

**TABLE 2. Decision table based on stimulus threshold values above (0) or below (1) 0.35 mA.<sup>3</sup>**

State	Electrode configuration				FN distance (mm)		Class
	Bipolar		Mono	Min	Max		
	$B_1$	$B_2$				$B_3$	Decision
0	0	0	0	0	0.4		Continue to drill
1	0	0	0	1			
2	0	0	1	1			
3	0	1	1	1	0.1	0.4	Further assessment
4	1	1	1	1	0	0.1	Abort RCI

thresholds are expected for the rest of configurations  $B_{2,3}$  and monopolar (larger volume conductors). For simplification of the look up table, the rest of theoretical (digital) scenarios (states) are neglected (e.g.,  $B_1(0)$ ,  $B_2(0)$ ,  $B_3(1)$ , Mono(0), *etc.*). Due to the existence of air cells and fluids in the mastoid during the RCI procedure, undesired spread of current could lead to higher stimulus thresholds in  $B_{2,3}$  or monopolar than in  $B_1$ . Table 2 only contains the five cases which are expected given the electrical properties of the probe in an assumed perfect volume conductor scenario. For a complete look up table refer to Weber *et al.*<sup>25</sup>

The surgeon verified the validity of the safety suggestion (Fig. 6, bottom panels) *via* secondary manual stimulation of the nerve at 0.3 mA ( $B_{1,2}$ ). If the FNM system suggests clearances from the trajectory to the FN between 0.1 and 0.4 mm, the surgeon should then make a decision go/no go based on the previous intraoperative imaging assessment. With remaining nerve clearances between 0.1 and 0.4 mm, no structural damage is expected to the facial nerve. However, a precise distance from the FN that ensures functional preservation (e.g., from factors such as thermal or vibrational interference) is not known.<sup>2,3</sup>

Upon verification of minimum safety distance margins of 0.4 mm to the facial nerve, the probe was retracted from the RCI tunnel and drilling was continued to the next FNM point. This process was repeated for each of the five FNM points ( $P_{1...5}$ ). When drilling of the facial recess was terminated, the trajectory reached the middle ear and stopped at a location (2 mm) in front of the cochlea. Free-running EMG was monitored for the remainder of the robotic drilling procedure and positive controls were recorded if required by the surgeon. Subsequently, cochlear access and CI electrode insertion was realized *via* an incision of the tympanic membrane (tympanomeatal flap), as described by Caversaccio *et al.*<sup>8</sup> Free-running EMG was monitored until the end of the procedure.

### *Electrophysiological Assessment of FN Function*

Facial nerve function was clinically and electrophysiologically assessed one day before surgery, and 11 days after surgery. Clinical assessment was performed by a senior physician at the department of neurology using the Sunnybrook scale.<sup>22</sup> For neurographic recordings, a Viking Select electromyography apparatus (Nicolet Biomedical, Madison, Wisconsin) was used with bandpass filtering from 10 Hz to 10 kHz. For surface recordings of the compound muscle action potential (CMAP) paired disk surface electrodes (Genuine Grass Silver electrodes, diameter 10 mm; Natus Medical Inc., Pleasanton, California, USA) with electrode gel were used. To assess facial symmetry, three recording sites were assessed in both sides of the face: (i) mentalis muscle (at the chin in a vertical line below the corner of the mouth), (ii) nasalis muscle (on the side of the bridge of the nose) and (iii) orbicularis oculi muscle (in a vertical line just below the corner of the eye). A reference electrode was placed on the tip of the nose. The facial nerve was stimulated along its anatomical course behind the jaw angle. Paired fixed surface electrodes (cathode-anode distance 20 mm) were used to apply a rectangular pulse (monophasic, 0.2 ms duration), and the stimulus intensity was adjusted to yield maximal responses. A ground electrode was placed between the stimulating and recording electrodes. Latency, amplitude and CMAP area for each side of the face and each of the three recorded muscles were reported

### *Data Analysis*

#### *FN Distance Assessment from Computer Tomography Scans*

Distance from the RCI trajectory to the facial nerve was assessed from postoperative computer tomography scans of the patient's mastoid, acquired one day after the RCI surgery (using the preoperative imaging protocol). To define the positions of the FNM points



in the RCI tunnel, co-registration of the postoperative and preoperative scans was performed *via* affine mutual information registration (Amira, FEI, Hillsboro, USA). After definition of an entrance and an exit cross-sections of the trajectory in the postoperative images, the RCI tunnel was linearly interpolated. Spatial positions of the measurement points ( $P_i$ ) along the segmented tunnel axis (DCL) were determined and the Euclidian distances from the trajectory to the FN ( $CD_i$ ) measured (Matlab, Mathworks, US). The Euclidian distance between the segmented drilled tunnel and the FN was defined as  $D_{FN}$  (Fig. 7b). The deviation (precision) of the measurement at the depth of the facial nerve was visually verified with the overlaid segmented tunnel in the postoperative image (observed variability of 1 voxel, i.e.,  $\pm 0.2$  mm).

#### *Extraction of Stimulus Thresholds and Facial Nerve Distance Mapping*

Electromyography responses to the stimulation pulses were examined in a 50-ms search window (20 kilosamples/s) leaving a 3-ms rejection period after the stimulation. The minimum current intensity that produced an EMG response ( $> 100 \mu\text{V}$ ) was defined as the stimulus threshold. For each trajectory, the stimulus thresholds of each stimulation channel were represented relative to a cross section of the FN in the plane containing  $D_{FN}$  (Fig. 4). Extracted values were compared to those calculated by the FNM intraoperatively.

## RESULTS

In all patients under study ( $n = 7$ ), the *positive control* and *free-running EMG* modules enabled continuous monitoring of the facial nerve activity during the procedure. In one case (patient 2), an unexpected problem with the intraoperative imaging system (imaging safety verification could not be assessed) led to conversion to CI mastoid surgery prior to stimulated FNM. This subject was not excluded from the study because secondary endpoints pertaining image-guided robotic drilling and free-running electromyography during the drilling process were obtained. In two cases (Patients 1, 5), one of the connections of the stimulating probe ( $A_3$ ) presented a high electrical impedance ( $Z_{A_3} > 20 \text{ k}\Omega$ ), which was later attributed to manufacturing error.

In the six patients who underwent a complete RCI procedure, sufficient distance between the RCI trajectory and the facial nerve was determined by the FNM system. In total, thirty stimulated FNM measurements (six patients  $\times$  five FNM points) were assessed. No high-energy or high-frequency neurotonic EMG activity bursts were observed in any of the patients while drilling through the facial recess. Low-energy EMG bursts were observed sporadically when drilling between FNM points or during manual surgical manipulation of the middle ear prior to accessing the cochlea (e.g., likely mechanical vibrations transmitted to the FN *via* the chorda tympani).

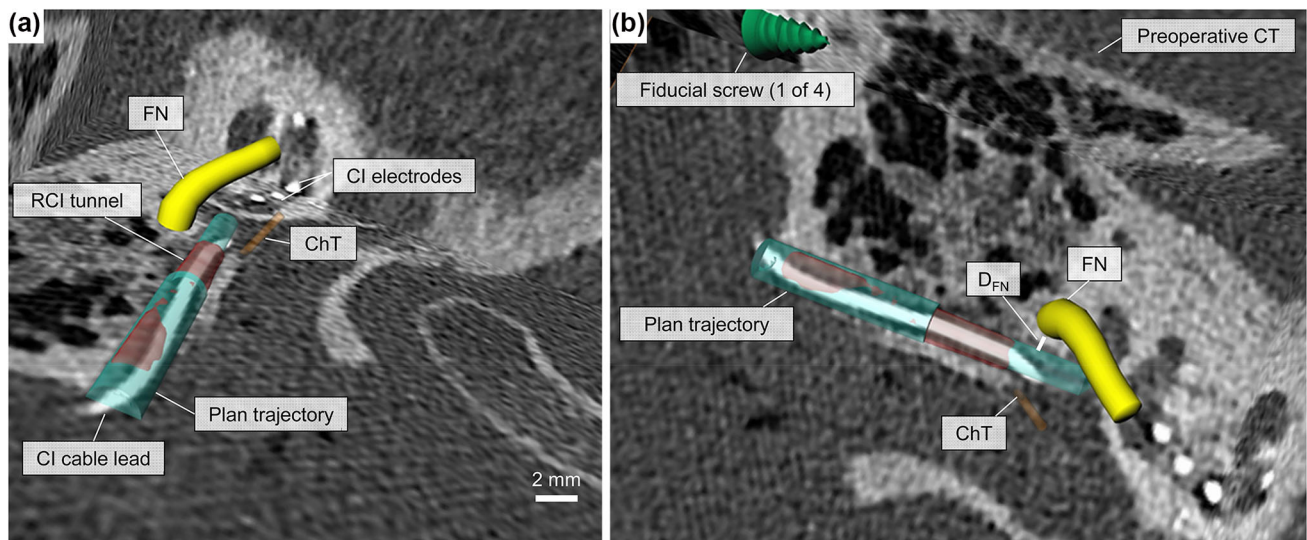


**FIGURE 7.** Robotic cochlear implantation drilled tunnel (Patient 5). The drilled tunnel (red) overlaps the planned trajectory (transparent sea blue). Sufficient distance margins to the preoperative plan are depicted with the distance ( $D_{FN}$ ) from the final trajectory to the facial nerve (yellow).

### Facial Nerve Distance Assessment Based on Stimulus Thresholds

For each trajectory, the multipolar stimulated FNM system determined *safe* passages with sufficient ( $> 0.4$  mm) distance to the FN (closest distance drill to facial nerve,  $CD_{1...5}$ ), as corroborated by postoperative measurement (Fig. 8). The trends of the stimulus thresholds correlated to the distance from the trajectory to the facial nerve, with larger thresholds required when the facial nerve lies further away from the trajectory. Overall, monopolar stimulation required significant lower stimulation intensities ( $\geq 0.4$  mA) than bipolar ( $B1 \geq 1.25$  mA) to elicit EMG responses (Table 3). In four of the six patients no EMG threshold response pertaining to the bipolar stimulation channel (B1) was observed for the maximum applied intensity (2.5 mA).

In Fig. 9, the scatter plot with all measured stimulus thresholds is depicted in relation to safe distance thresholds (green rectangle). The stimulus threshold values measured with the configurations of the probe  $B_2$  and  $B_3$  were similar (10/16 stimulus thresholds for  $B_2$  were the same as for  $B_3$ ). The proposed FNM system correctly classified the safety of the facial nerve to drill tunnel distance ( $CD_i > 0.4$  mm) in all cases.

### Preoperative and Postoperative Assessment of Facial Nerve Function

Postoperative Sunnybrook scale scores were unchanged from preoperative values in all patients. Two patients had a reduced score pre- and post-operatively (80/100, Patient 1; and 96/100, Patient 3) on the planned implantation side due to previous idiopathic facial paresis as revealed by patient history. Neurographic recordings of the facial nerve revealed no significant differences between sides for all assessed parameters (latency, amplitude and area of CMAP) before and after surgery (Table 4).

## DISCUSSION

Within this work the first clinical findings of a multimodal FNM approach to facial nerve safety assessment during RCI has been presented. Results from the first RCI clinical cases demonstrated that the approach could reliably detect a safe drill trajectory with respect to facial nerve distance. Observed minimum stimulus thresholds confirmed safety distance margins derived from an animal model (0.4 mm with stimulus thresholds  $\geq 0.3$  mA for the bipolar configuration  $B_{1,2}$ ).<sup>3</sup> The deployed neuromonitoring system and method aided the surgeon to confirm *safe* drilling

passages and enabled continuous monitoring of the nerve activity during image-guided robotic cochlear implantation.

The developed FNM RCI system and approach is based on a multipolar stimulating methodology, a positive control stimulation channel and free-running electromyography. The stimulating FNM approach demonstrated effective monopolar and bipolar stimulation of the facial nerve within ranges suitable for RCI procedures. The FNM safety assessment was able to discriminate sufficient safety distance from the drilled trajectory ( $> 0.39$  mm). The stimulation thresholds validated during the first RCI cases are in agreement with values determined from preclinical studies in an animal model<sup>3</sup> for lateral distances above 0.4 mm. The performance of the FNM approach at the critical distance range ( $< 0.2$  mm) could not be evaluated during the first RCI cases as this would represent an undesired clinical situation that would place the facial nerve at risk. For this reason, clinical validation of potentially critical drilling distance detection remains challenging.

During standard cochlear implant surgery or other types of mastoidectomy, milling a large cavity of bone and irrigating at the same time, results in a large bath of conducting fluids surrounding the facial recess. In practice, spread of stimulating current leads to reduced or absence of EMG response, which can be avoided or minimized by using flushed insulated electrodes as proposed by Kartush *et al.*<sup>15</sup> During RCI, it is expected that the added (NaCl, 0.9%) solution will create an electrically conducting micro-film (few micrometers) between the cathode tip and the surrounding bony material. Therefore, minimal current spread leading to reduction or cancellation of EMG responses is expected. In the future, suctioning any remaining fluids in the RCI tunnel before insertion of the stimulating probe could be investigated to assess its influence in sensitivity and specificity of facial nerve proximity estimation.

In 2/6 patients (patients 5,6) the same (postoperative) distance from the trajectory to the facial nerve led to different stimulus threshold patterns. This suggests that the patient specific electrical properties influence the intensity required to stimulate the nerve, as described in preclinical validations.<sup>3</sup> Balmer *et al.* carried out a pilot study to characterize the electrical properties of the mastoid bone.<sup>5</sup> Electrical properties of the tissue surrounding the trajectory measured *via* impedance spectroscopy may, in the future, enable calibration of the facial nerve distance assessment based on FNM during RCI.

The precision of the postoperative assessment of distance from the RCI drilled tunnel to the facial nerve is limited. Variations within one voxel ( $\pm 0.2$  mm) in

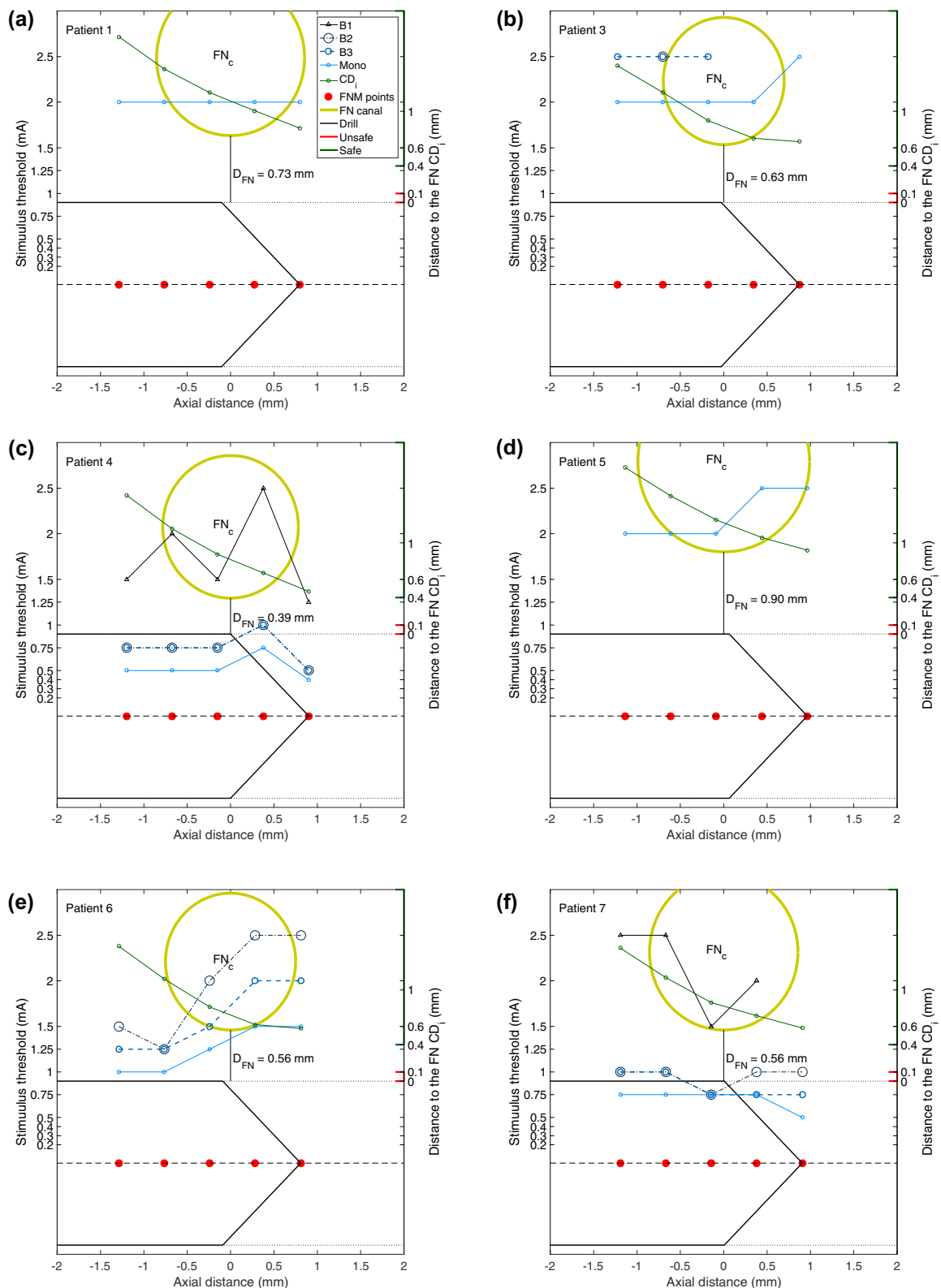


**FIGURE 8.** Stimulus thresholds relative to the facial nerve per each of the RCI drilled trajectories (postoperative). The drill at the last measurement point is depicted (black polyline). On the y-left-axis the intensity (milliamp) is represented. In the y-right-axis (green curve), the postoperative distance from the tunnel to the FN (CD<sub>1</sub>) at each FNM measurement point is depicted. The yellow circle represents the cross section of the preoperative facial nerve (plan) at the plane of minimum distance from the final trajectory to the FN in the postoperative co-registered drilled trajectory.

the postop images were observed (results not reported) at the depth of the facial nerve by segmenting entry and target cross sections in different attempts. Recently, a method to accurately assess distances from the drill trajectory to the facial nerve based on the intraoperative image of the position of the drilled tunnel before reaching the facial nerve has been validated.<sup>20</sup> In the future, this method could be used to assess distance from the trajectory to the facial nerve for comparison of safety distance margins suggested by the FNM approach.

Free-running EMG presents limited information during the procedure. Interpretation of EMG bursts, e.g., indicating unexpected hazardous drilling may be challenging if not facilitated *via* integrated signal detection algorithms. A hazardous physical condition during RCI, e.g., high temperature during drilling,<sup>18</sup> may trigger a neurotonic discharge. If this EMG triggered signal can be effectively detected (milliseconds), a warning-signal could immediately be sent to stop operation of the image-guided drill system. Extensive preclinical evaluation would be necessary to demonstrate its potential efficacy to detect temperature evoked EMG.

In the present study, the stimulus threshold values measured with the configurations of the probe B<sub>2</sub> and B<sub>3</sub> were similar. This suggests that the configuration B<sub>3</sub> might not add significantly different information than B<sub>2</sub>. In the future, the number of channels in the stimulating probe (B<sub>1</sub>, B<sub>2</sub>, B<sub>3</sub>) could be reduced from three to two (no B<sub>3</sub>) without significantly reducing the range of FN distance discrimination (> 0.4 mm). This hypothesis could be studied using finite element models to simulate the electrical field as a function of stimulating intensity using the CT data of the patient’s mastoid.<sup>2,5</sup>

Although the presented discretized FNM approach enables *safe* and *unsafe* distance margins to be discriminated during RCI, use of a stimulating probe implies limited spatial resolution. The axial distance resolution was empirically defined as 0.5 mm with five

measurement points linearly distributed along 2 mm, the maximum expected facial nerve diameter.<sup>24</sup> To further increase the spatial resolution of the neuromonitoring method before reaching the facial nerve, a logarithmic incremental function could be used, as a factor of the preoperative lateral distance from the trajectory to the facial nerve. Furthermore, a drill-integrated stimulating approach could enable in the future safer RCI drilling and reduction of workflow complexity,<sup>1</sup> combining an enhanced spatial and temporal resolution.

In conclusion, an application specific nerve monitoring approach for minimally invasive robotic drilling of an access tunnel to the cochlea has been developed and applied in a first clinical trial. Measurements performed automatically at preoperatively defined distances from the facial nerve could be used to determine safety of the drill trajectory intraoperatively. The presented system and analysis correctly determined suffi-

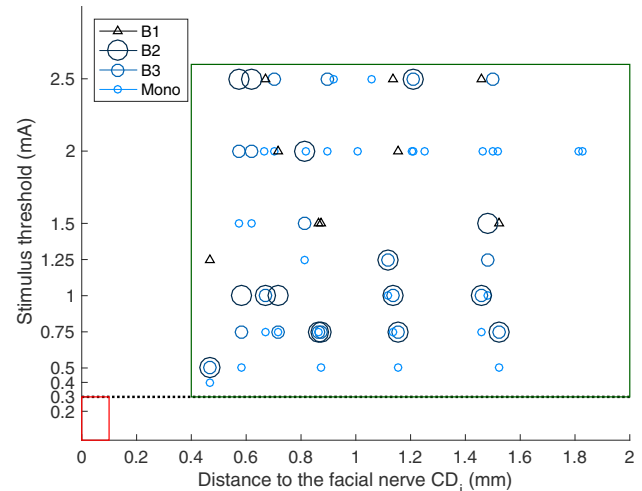


**FIGURE 9.** Scatter plot with all stimulation measurement points (six patients × five FNM points) as a function of drill-to-FN distance CD<sub>1</sub>. All stimulus thresholds-to-facial nerve distance measured paired points fall within the predefined *safe* distance margin (green, FN distance > 0.4 mm).<sup>3</sup>

**TABLE 3.** The minimum stimulus thresholds and the determined facial nerve distance per tunnel.

Subject	Minimum stimulus threshold				Preop D <sub>FN</sub> (mm)	FNM CD <sub>5</sub> (mm)	Postop	
	B <sub>1</sub> (mA)	B <sub>2</sub> (mA)	B <sub>3</sub> (mA)	Mono (mA)			CD <sub>5</sub> (mm)	D <sub>FN</sub> (mm)
1	NR	NR	HZ	2	0.73	> 0.4	0.82	0.73
3	NR	2.5	2.5	1.5	0.62	> 0.4	0.67	0.63
4	1.3	0.5	0.5	0.4	0.54	> 0.4	0.47	0.39
5	NR	NR	HZ	2	0.72	> 0.4	0.92	0.90
6	NR	1.5	1.3	1	0.65	> 0.4	0.58	0.56
7	1.5	0.8	0.8	0.5	0.50	> 0.4	0.58	0.56

NR: no EMG response above threshold at maximum applied intensity of 2.5 mA. HZ: high impedance ( $Z > 20$  k $\Omega$ ) at stimulating electrode configuration (technical problem).

**TABLE 4. Preop- and postoperative recording sites and side differences (mean and SD).**

EMG parameter	Recording site of CMAP	Relative side difference (%)		Wilcoxon signed-rank-test
		Preoperative mean (SD)	Postoperative mean (SD)	
Latency (ms)	Mentalis	− 1 (20)	− 1 (28)	n.s.
	Nasalis	− 5 (20)	− 6 (22)	n.s.
	Orbicularis oculi	− 14 (27)	− 4 (7)	n.s.
Amplitude (mV)	Mentalis	7 (29)	− 8 (35)	n.s.
	Nasalis	8 (23)	6 (13)	n.s.
	Orbicularis oculi	− 4 (49)	− 6 (23)	n.s.
Area (mV <sub>rms</sub> )	Mentalis	− 7 (33)	− 7 (22)	n.s.
	Nasalis	4 (30)	6 (10)	n.s.
	Orbicularis oculi	0 (40)	7 (21)	n.s.

CMAP, compound muscle potential; SD, standard deviation; n.s., no significant difference.

cient safety distance margins (> 0.4 mm) to the facial nerve in all cases. This safety approach could be translated into surgical scenarios where image-guided robotically drilled trajectories are required in the proximity of delicate nerves (e.g., robotic spine surgery).

#### ACKNOWLEDGMENTS

The authors thank Laetitia Racz-Perroud, Fabian Zobrist and Marco Matulic (CAscination AG) for technical support. The authors thank Dr. Thilo Krüger and Celine Wegner (inomed GmbH) for technical support. Dr. Thomas Wyss-Balmer contributed with electrical modeling of the presented stimulation probe. Surgical photographs are attributed to Gianni Paucello.

#### CONFLICT OF INTEREST

This work was supported by the Swiss Commission for technology and innovation (Project MIRACI 17618.1), the Swiss National Science Foundation (Project 205321\_176007), by MED-EL GmbH (Innsbruck, Austria) and CAscination AG (Bern, Switzerland).

#### REFERENCES

- Anso, J., K. Gerber, S. Weber, K. Thorwarth, A. Chacko, and J. Patscheider. Intervention Device with Electrodes, P5324EP00, 2018.
- Anso, J., et al. Electrical impedance to assess facial nerve proximity during robotic cochlear implantation. *IEEE Trans. Biomed. Eng.* 1–1, 2018.
- Ansó, J., et al. A Neuromonitoring approach to facial nerve preservation during image-guided robotic cochlear implantation. *Otol. Neurotol.* 37(1):89–98, 2016.
- Ansó, J., et al. Feasibility of using EMG for early detection of the facial nerve during robotic direct cochlear access. *Otol. Neurotol.* 35(3):545–554, 2014.
- Balmer, T. W., et al. In-vivo electrical impedance measurement in mastoid bone. *Ann. Biomed. Eng.* 45(4):1122–1132, 2017.
- Bell, B., et al. In vitro accuracy evaluation of image-guided robot system for direct cochlear access. *Otol. Neurotol.* 34:1284–1290, 2013.
- Bernardeschi, D., et al. Continuous facial nerve stimulating burr for otologic surgeries. *Otol. Neurotol.* 32(8):1347–1351, 2011.
- Caversaccio, M., et al. Robotic cochlear implantation: surgical procedure and first clinical experience. *Acta Otolaryngol.* 137(4):447–454, 2017.
- Choung, Y. H., K. Park, M. J. Cho, P. H. Choung, Y. R. Shin, and H. Kahng. Systematic facial nerve monitoring in middle ear and mastoid surgeries: ‘surgical dehiscence’ and ‘electrical dehiscence’. *Otolaryngology* 135(6):872–876, 2006.
- Gerber, N., B. Bell, K. Gavaghan, C. Weisstanner, M. D. Caversaccio, and S. Weber. Surgical planning tool for robotically assisted hearing aid implantation. *Int. J. Comput. Assist. Radiol. Surg.* 9(1):11–20, 2014.
- Gerber, N., et al. High accuracy patient-to-image registration for the facilitation of image guided robotic microsurgery on the head. *IEEE Trans. Biomed. Eng.* 60(4):960–968, 2013.
- Heman-Ackah, S. E., S. Gupta, and A. K. Lalwani. Is facial nerve integrity monitoring of value in chronic ear surgery? *Laryngoscope* 123(1):2–3, 2013.
- Holland, N. R. Intraoperative electromyography. *J. Clin. Neurophysiol.* 19(5):444–453, 2002.
- Hormes, J., and J. Chappuis. Monitoring of lumbosacral nerve roots during spinal instrumentation. *Spine (Phila. Pa. 1976)* 18(14):2059–2062, 1993.
- Kartush, J. M., J. K. Niparko, S. C. Bledsoe, M. D. Graham, and J. L. Kemink. Intraoperative facial nerve monitoring: a comparison of stimulating electrodes. *Laryngoscope* 95(12):1536–1540, 1985.
- Kim, S. M., S. H. Kim, D. W. Seo, and K. W. Lee. Intraoperative neurophysiologic monitoring: basic principles and recent update. *J. Korean Med. Sci.* 28(9):1261–1269, 2013.

- <sup>17</sup>Labadie, R. F., J. H. Noble, B. M. Dawant, R. Balachandran, O. Majdani, and J. M. Fitzpatrick. Clinical validation of percutaneous cochlear implant surgery: initial report. *Laryngoscope* 118(6):1031–1039, 2008.
- <sup>18</sup>Labadie, R. F., *et al.* Minimally invasive image-guided cochlear implantation surgery: first report of clinical implementation. *Laryngoscope* 124(8):1915–1922, 2014.
- <sup>19</sup>Owen, J., *et al.* The use of mechanically elicited electromyograms to protect nerve roots during surgery for spinal degeneration. *Spine (Phila. Pa. 1976)* 19(15):1704–1710, 1994.
- <sup>20</sup>Rathgeb, C., *et al.* The accuracy of image based safety analysis for robotic cochlear implantation. *Int. J. Comput. Assist. Radiol. Surg.*
- <sup>21</sup>Roland, A. P. S., C. Editor, and A. D. Meyers. Principles of Electrophysiologic Monitoring, pp. 1–9, 2012.
- <sup>22</sup>Ross, B. G., G. Fradet, and J. M. Nedzelski. Development of a sensitive clinical facial grading system. *Otolaryngol. Head. Neck Surg.* 114(3):380–386, 1996.
- <sup>23</sup>Silverstein, H., and S. Rosenberg. Intraoperative facial nerve monitoring. *Otolaryngol. Clin. N. Am.* 24(3):709–725, 1991.
- <sup>24</sup>Vianna, M., *et al.* Differences in the diameter of facial nerve and facial canal in bell’s palsy—a 3-dimensional temporal bone study. *Otol. Neurotol.* 35(3):514–518, 2014.
- <sup>25</sup>Weber, S., *et al.* Instrument flight to the inner ear. *Sci. Robot.* 2(4):eaal4916, 2017.
- <sup>26</sup>Williamson, T., *et al.* Population statistics approach for safety assessment in robotic cochlear implantation. *Otol. Neurotol.* 38(5):759–764, 2017.